Applied Thermal Engineering 80 (2015) 76–86

Contents lists available at ScienceDirect

Applied Thermal Engineering

journal homepage: www.elsevier.com/locate/apthermeng

Research paper

An experimental study of two-phase pressure drop of acetone in triangular silicon micro-channels

Yunhua Gan [a], Jinliang Xu [b, *], Yuying Yan [c, *]

[a] School of Electric Power, South China University of Technology, Guangdong 510640, China
[b] School of Energy, Power and Mechanical Engineering, North China Electric Power University, Beijing 102206, China
[c] Energy and Sustainability Research Division, Faculty of Engineering, University of Nottingham, University Park, Nottingham NG7 2RD, UK

HIGHLIGHTS

- Two-phase pressure drop in silicon micro-channels was measured under high outlet quality conditions.
- The homogeneous model and the separated flow model are compared with the present data.
- Several correlations for macro-scale and mini/micro-scale channels are estimated.
- A new correlation is developed using a modified Chisholm model.

ARTICLE INFO

Article history:
Received 20 October 2014
Accepted 13 January 2015
Available online 22 January 2015

Keywords:
Silicon micro-channel
Flow boiling
Two-phase pressure drop

ABSTRACT

Two-phase pressure drop was measured across a silicon micro-channels heat sink. Ten triangular micro-channels were fabricated in a silicon substrate by the etching technique in a silicon substrate. Each micro-channel is 300 μm in width and 212 μm in depth, forming the hydraulic diameter of 155.4 μm. Experimental studies were performed with acetone as working fluid under the following conditions: inlet pressure of P_{in} = 1.3–1.6 bar, inlet temperature T_{in} = 23.0–39.1 °C, mass velocity of G = 65.52 –289.61 kg/m^2 s, outlet quality of $x_{e,out}$ = 0.38–superheat, and heat flux of q = 141.92–481.08 kW/m^2. The frictional pressure drop during flow boiling is estimated using two models, namely the homogeneous model and the separated flow model. In addition, the measured pressure drops are compared with those from a few correlation models available for macro-scales and mini/micro-scales. A new correlation is developed based on the Chisholm constant B as a function of mass flux. It is found that the new correlation can be used to predict the present experimental data within a mean absolute error (MAE) of 12.56%.

1. Introduction

In the last decade, heat transfer and pressure drop in micro system received more and more attention. Flow boiling is a highly efficient mode of heat transfer at micro scale [1–3]. Flow boiling in micro-channels has many advantages, such as very uniform chip temperatures distribution [4].

Although in general the pressured drop across micro-channel heat sinks may become very high when the hydraulic diameter is reduced, the results of both heat transfer enhancement and pressure drop reduction were achieved by the new design in single-phase heat transfer process [5]. However this may not be successful under two-phase flow boiling condition. Thus, in order to design micro-channel heat sinks with high performance, the accurate prediction of two-phase pressure drop is very important.

Yu et al. [6] performed experimental study of water on two-phase pressure drop in a small horizontal tube and modified the Chisholm two-phase multiplier correlation to better predict their data. Sun and Mishima [7] collected 2092 data from 18 published papers using 12 kinds of working fluids, evaluated 11 correlations and models for calculating the two-phase frictional pressure drop, and also proposed a modified Chisholm correlation with better agreement in turbulent region.

Lee and Garimella [8] paid a great attention on the channel size effect, and applied regression analysis to obtain a new correlation of

* Corresponding authors.
E-mail addresses: xjl@ncepu.edu.cn (J. Xu), yuying.yan@nottingham.ac.uk (Y. Yan).

http://dx.doi.org/10.1016/j.applthermaleng.2015.01.038
1359-4311/

Nomenclature

B	parameter in Chisholm correlation
C	coefficient in empirical correlations
c_{pf}	specific heat (J/kg K)
d_h	hydraulic diameter of the micro-channel (m)
f	friction factor
f_f	liquid friction factor
f_g	vapour friction factor
f_{tp}	two phase friction factor
G	mass flux (kg/m^2 s)
h	enthalpy (J/kg)
h_f	enthalpy of liquid (J/kg)
h_{fg}	latent heat of vaporization (J/kg)
k_f	thermal conductivity of liquid (W/m K)
k_g	thermal conductivity of vapour (W/m K)
L	length of micro-channels (m)
L_1	length to reach quality of unity (m)
L_c	length of inlet header (m)
L_e	length of outlet header (m)
L_h	effective heating length (m)
L_{in}	length before heating in the micro-channel (m)
$L_{sp,f}$	length of single-phase liquid flow area (m)
$L_{sp,g}$	length of single-phase vapour flow area (m)
L_{tp}	length of two-phase flow area (m)
L_{out}	length after heating in the micro-channel (m)
m	mass flow rate (kg/s)
MRE	mean relative error
N	number of data points
N_{conf}	confinement number
P_{in}	inlet pressure (Pa)
ΔP	pressure drop for the heat sink with the micro-channels (Pa)
ΔP_c	pressure drop due to contraction (Pa)
ΔP_e	pressure drop due to expansion (Pa)
ΔP_{exp}	experimental pressure drop (Pa)
ΔP_L	pressure drop across the micro-channels (Pa)
ΔP_{L_h}	pressure drop across the heating area (Pa)
ΔP_{in}	pressure drop across the length before heating in the micro-channel (Pa)
ΔP_{out}	pressure drop across the length after heating in the micro-channel (Pa)
ΔP_{pred}	predicted pressure drop (Pa)
$\Delta P_{sp,f}$	single-phase liquid pressure drop (Pa)
$\Delta P_{sp,g}$	single-phase vapour pressure drop (Pa)
ΔP_{tot}	pressure drop for the heat sink measured by the differential pressure transducer (Pa)
$\Delta P_{tp,f}$	two-phase frictional pressure drop (Pa)
$\Delta P_{tp,g}$	two-phase accelerational pressure drop (Pa)
Q	effective heating power (W)
q	effective heat flux based on the side wall channel area (W/m^2)
Re	Reynolds number
Re_f	liquid Reynolds number
Re_{fo}	liquid Reynolds number assuming total flow flowing as liquid only
Re_{tp}	two-phase mixture Reynolds number
T_f	fluid temperature (°C)
T_{in}	inlet liquid temperature (°C)
T_{sat}	saturated temperature (°C)
T_w	chip temperature (°C)
W	width of thin film heater (m)
We_{fo}	Weber number assuming total fluid flowing as liquid only
X	Martinelli parameter
X_{vv}	Martinelli parameter based on laminar liquid-laminar vapour flow
X_{vt}	Martinelli parameter based on laminar liquid-turbulent vapour flow
x_e	thermodynamic equilibrium quality
$x_{e,out}$	exit vapour quality
y	coordinate along flow direction (m)
z	coordinate along width direction (m)

Greek symbols

α	void fraction
α_{out}	exit void fraction
I^2	dimensionless physical property coefficient
μ_f	liquid viscosity (Pa s)
μ_g	vapour viscosity (Pa s)
μ_{tp}	two-phase mixture viscosity (Pa s)
ρ_f	liquid density (kg/m^3)
ρ_g	vapour density (kg/m^3)
σ	surface tension (N/m)
ω	volumetric quality
ϕ_f^2	two-phase frictional multiplier based on local liquid flow rate
ϕ_{fo}^2	two-phase frictional multiplier based on total flow considered as liquid

Subscripts

a	accelerational
c	contraction
e	expansion
exp	experimental
f	liquid; frictional
fo	total flow assumed liquid phase
g	vapour
h	heating film
in	inlet
out	outlet
pred	predicted
sat	saturated
sp	single-phase
tot	total
tp	two-phase
w	chip wall

pressure drop for saturated boiling of water. Phan et al. [9] observed that the total two-phase pressure drop of water significantly increases with static contact angle. Brutin et al. [10] found that the pressure drops for two-phase flow in microgravity are significantly higher than that for single-phase flow under similar conditions. Fu et al. [11] performed an experimental study on the pressure drop of ethanol–water mixtures in a diverging micro-channel with artificial cavities, and put forward a new correlation based on boiling number, Weber number, and Marangoni number.

Different researchers used channels with different geometry, material, or hydraulic diameter, and carried out experiments with different working fluids under dissimilar conditions. So it is a very difficult work to develop a universal prediction correlation. Ribatski et al. [12] reviewed the experimental results, carried out

comparisons using 12 prediction methods, and found that these methods work poorly for vapour qualities higher than 0.5 where annular, partial dryout and mist flow patterns would be expected.

However it seems that the tools are not suitable for the present experimental data, using acetone in triangular silicon micro-channels with hydraulic diameter of 155.4 μm under high mass quality conditions. The measured two-phase frictional pressure drops are compared with those from a few correlation models available for macro-scales and mini/micro-scales channels. The major aim of the present study is to develop a new correlation with better predictive accuracy.

2. Experimental system

Fig. 1 shows the experimental setup using a micro-channel heat sink. The working fluid used in the present study is pure acetone, which has a low saturated boiling temperature of 56.29 °C at 1 bar. Liquid acetone is pushed by high pressure N_2, flows through a 2 μm filter, the micro-channel test section, the heat exchanger, and into the container. The inlet pressure of the test section is controlled by a high precision pressure regulator. The acetone temperature in the tank is maintained by a PID constant temperature control unit with the uncertainty of ±0.5 °C. The inlet and outlet temperatures were measured by high precision K type jacket thermocouples with the uncertainty of ±0.4 °C. The inlet fluid pressure was measured by a pressure transducer (Model 206, Setra Systems, Inc.) with the uncertainty of ±1%. A differential pressure transducer (Senex) was used to measure the pressure drop across the micro-channel test section with the uncertainty of ±0.1%. All these signals were collected by a HP Agilent 34970A data acquisition unit. The liquid acetone was heated by a Pt thin film heater to start boiling, and then cooled by a water heat exchanger. The mass flux of condensed liquid acetone was measured by a high precision electronic balance during a long period of time with the uncertainty of ±0.02 g.

Fig. 2(a) shows the primary components of the test section, i.e. a transparent Pyrex glass cover plate, a parallel silicon micro-channels substrate, and a Pt thin film heater. The glass cover is 30 mm in length, 7 mm in width, and 0.410 mm in thickness. The silicon substrate is 0.530 mm in thickness. Ten parallel triangular micro-channels with 21.450 mm in length were etched and central located in the silicon substrate. Each micro-channel is 0.300 mm in width, 0.212 mm in depth, forming the hydraulic diameter of 155.4 μm. The whole width of ten micro-channels is 4.35 mm. The glass cover was bonded with the silicon substrate. A Pt thin film heater was deposited on the back of the silicon substrate of 4.2 mm in width and 16 mm in length. The heater is driven by an AC power supply with a common 50 Hz frequency to provide a uniform heat flux.

Fig. 2(b) shows the dimensions and relative positions of the flow view area, the micro-channel area, the whole chip area, and the heating area. 2D coordinates is shown in the heating area with z as the flow direction and y as perpendicular to z. A combined optical system consists of a Leica M sterio-microscope (Germany) and a Redlake MASD MotionXtra HG-100 K high speed camera (USA) is employed to observe the boiling flow pattern in the micro-channels in the flow view area (6.45 mm × 4.35 mm). A high resolution, high accuracy infrared radiation imaging system (FLIR ThermaCAM SC3000 IR) is used to measure the temperatures of the chip thin film. The IR camera has a thermal sensitivity of 0.02 K at 303 K, a spatial resolution of 1.1 mrad, and a typical resolution of 320 × 240 pixels. In order to ensure the accuracy of measurement, a very thin “black lacquer” was uniformly painted on the surface of the thin film heater, which can reach an emissivity of approximately 0.94. After calibration, the uncertainty of chip temperature measurement is within ±0.4 °C. The IR camera measured image files and corresponding data files which contain 6080 data points related to the heating area (16.000 mm × 4.200 mm) all is stored by a PC.

Before the boiling heat transfer experiment, all transducers were calibrated, and single-phase liquid flow and heat transfer was performed using a round steel tube as test section with the inner diameter of 6 mm. All the results were compared with classical correlations for pressure drop in macro scale with acceptable errors. Then the experiments using silicon micro-channels were carried out based on the validated experimental system.

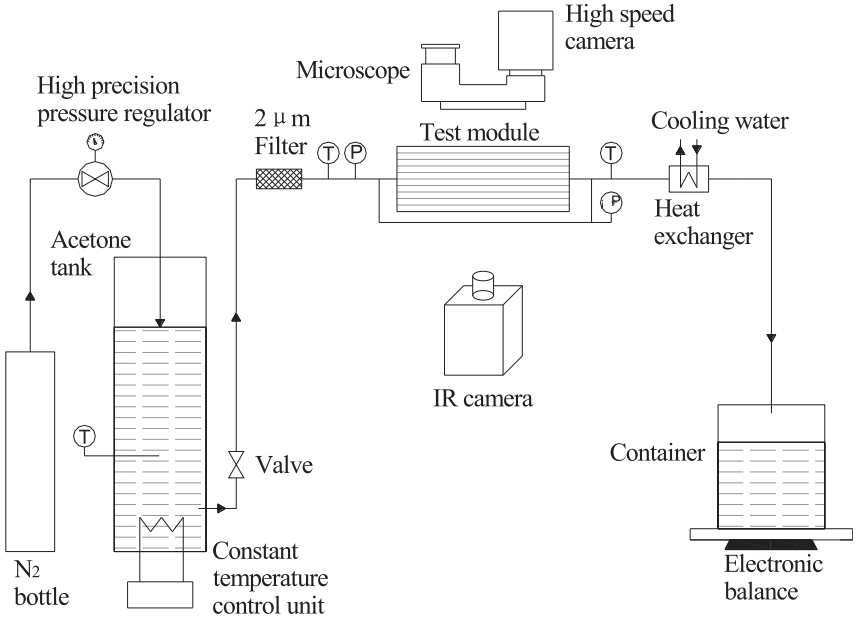

Fig. 1. The experimental system.

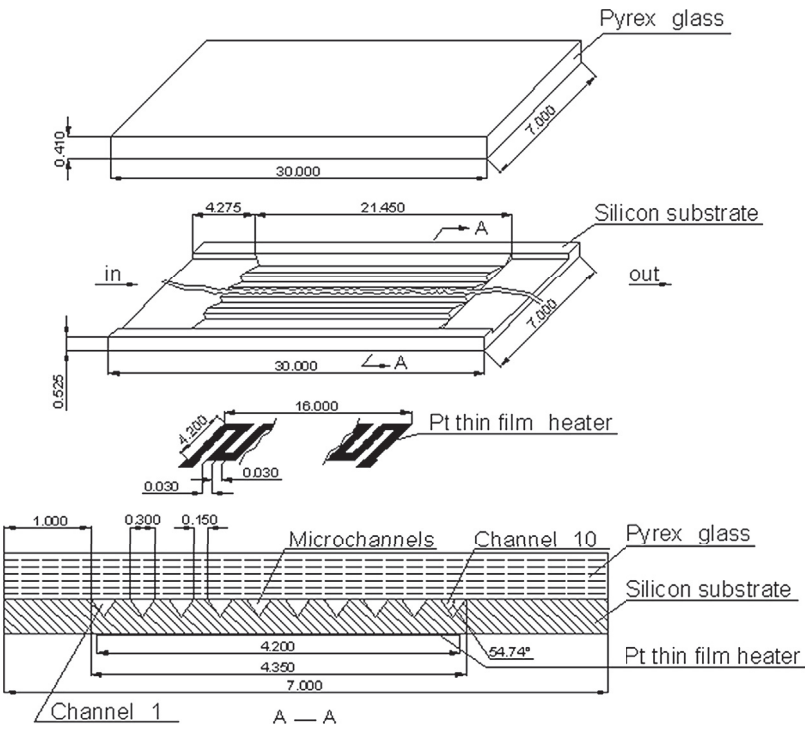

(a)

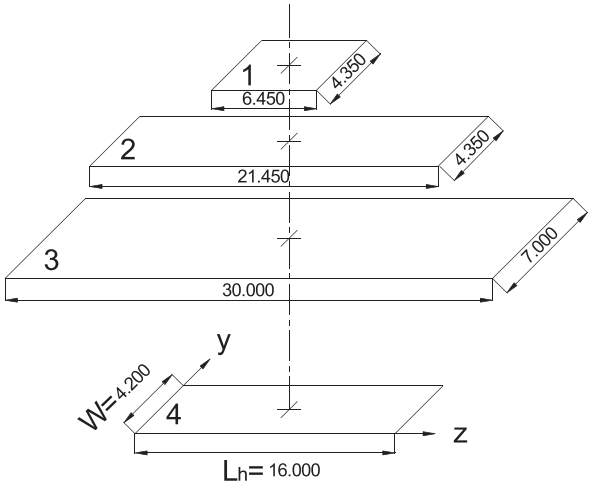

(b)

Fig. 2. Silicon micro-channel test section. 1: Flow view area, 2: Micro-channels area, 3: Whole silicon chip, 4: Effective thin film heater (all dimensions are in mm).

Table 1
Physical properties of acetone at 1 bar saturated condition.

Properties	Unit	Value
T_{sat}	°C	56.29
ρ_f	kg/m^3	748.01
c_{pf}	J/(kg K)	2302.5
h_{fg}	J/kg	512.94
σ	N/m	0.0192
μ_f	Pa s	2.37×10^{-4}
μ_g	Pa s	8.31×10^{-6}
k_f	W/(m K)	0.518
k_g	W/(m K)	0.0136

Table 2
Experimental uncertainty.

Parameters	Uncertainty	Parameters	Uncertainty
G	0.2%	q	6.5%
m	0.2%	Re	1.71%
P_{in}	1.0%	T_f	1.7% (0.4 °C)
ΔP	0.1%	T_w	1.1% (0.4 °C)
Q	6.5%	x_e	8.9%

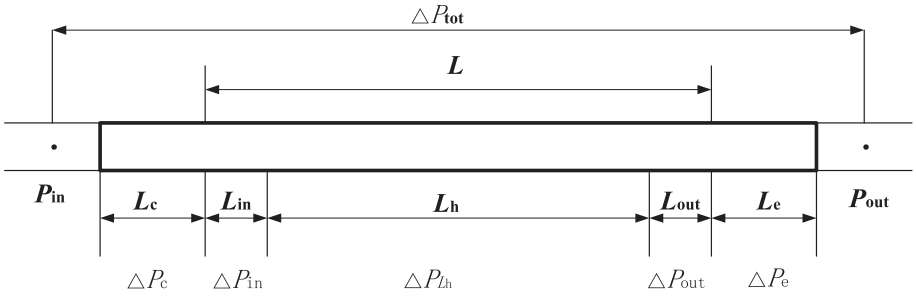

Fig. 3. Schematic of flow regions in the whole test section.

Table 3
Lengths of the heat sink.

Properties	Unit	Value
L	mm	21.450
L_c	mm	4.275
L_{in}	mm	2.725
L_h	mm	16.000
L_{out}	mm	2.725
L_e	mm	4.275

Table 4
Micro-channel heat sink pressure drop components.

Components	Equations
ΔP_c	$\Delta P_c = 0.6332\ G^2/\rho_f$
ΔP_{in}	$\Delta P_{in} = (2L_{in}\cdot f_f\cdot G^2)/(d_h\cdot\rho_f)$ $Re_f = Gd_h/\mu_f$, $f_f = 13.311/Re_f$
$\Delta P_{sp,f}$	$\Delta P_{sp,f} = (2L_{sp,f}\cdot f_f\cdot G^2)/(d_h\cdot\rho_f)$ $Re_f = Gd_h/\mu_f$, $f_f = 13.311/Re_f$
$\Delta P_{sp,g}$	$\Delta P_{sp,g} = (2L_{sp,g}\cdot f_g\cdot G^2)/(d_h\cdot\rho_g)$ $Re_g = Gd_h/\mu_g$, $f_g = 13.311/Re_g$
ΔP_{out}	$\Delta P_{out} = 2f_{tp}\ G^2 L_{out}\ (1+(\rho_f/\rho_g-1)x_{e,out})/(d_h\ \rho_f)$ $Re_{tp} = Gd_h/\mu_{tp}$, $f_{tp} = 13.311/Re_{tp}$ $1/\mu_{tp} = x_e/\mu_g+(1-x_e)/\mu_f$
ΔP_e	$\Delta P_e = 0.2244\ G^2(1+(\rho_f/\rho_g-1)x_{e,out})/\rho_f$

3. Results and discussion

3.1. Pressure drop determination

Pure acetone (CH_3COCH_3, purity >99.5%) is employed as working fluid in the experimental study. The physical properties of saturated acetone at 1 bar are shown in Table 1.

The physical properties of acetone at different temperature are calculated based on the equations available in Ref. [13]. 56 runs of two-phase frictional pressure drop experiments were performed, and the operating conditions for this study were as follows: inlet pressure of $P_{in} = 1.3–1.6$ bar, inlet temperature $T_{in} = 23.0–39.1$ °C, mass velocity of $G = 65.52–289.61$ kg/m^2 s, outlet quality of $x_{e,out} = 0.38$–superheat, and heat flux of $q = 141.92–481.08$ kW/m^2. The important parameter uncertainties are summarized in Table 2.

Fig. 3 shows the flow regions in whole test section which is described in Fig. 2. Acetone was supplied into the inlet tube, the inlet header L_c, the micro-channels section L, outlet header L_e and outlet tube. And the micro-channels section was divided into inlet section L_{in}, heating section L_h and outlet section L_{out}. All lengths of these flow regions are shown in Table 3. The inlet pressure P_{in} and the total pressure drop across the test section ΔP_{tot} were measured by a pressure transducer and a differential pressure transducer respectively. The total pressure drop is the sum of pressure drops across the inlet header, micro-channels, outlet header, as well as pressure losses and recoveries associated with the contractions and expansions respectively. Neglecting the pressure drops from the pressure measurement point to the inlet and outlet of the test section, the total pressure drop can be expressed as into inlet section L_{in}, heating section L_h and outlet section L_{out}. All lengths of these flow regions are shown in Table 3. The inlet pressure P_{in} and the total pressure drop across the test section ΔP_{tot} were measured by a pressure transducer and a differential pressure transducer respectively. The total pressure drop is the sum of pressure drops across the inlet header, micro-channels, outlet header, as well as pressure losses and recoveries associated with the contractions and expansions respectively. Neglecting the pressure drops from the pressure measurement point to the inlet and outlet of the test section, the total pressure drop can be expressed as

$$\Delta P_{tot} = \Delta P_c + \Delta P_L - \Delta P_e = \Delta P_c + \Delta P_{in} + \Delta P_{L_h} + \Delta P_{out} - \Delta P_e. \quad (1)$$

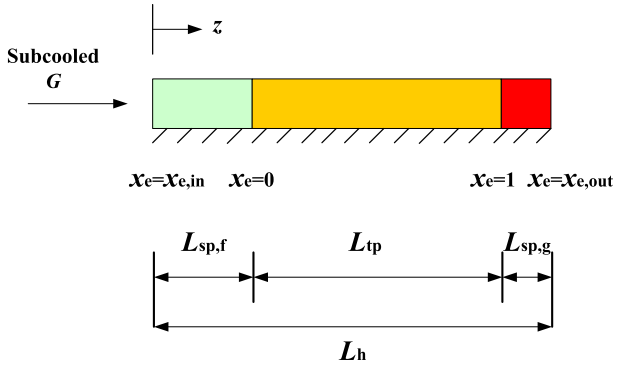

Fig. 4. Schematic of flow regions in a micro-channel.

Table 5
Two-phase mixture viscosity models adopted in the HEM.

$\Delta P_{tp,f} = 2f_{tp}\ G^2\ L_{tp}(1+0.5\times(\rho_f/\rho_g-1)x_{e,out})/(d_h\rho_f)$
$Re_{tp} = Gd_h/\mu_{tp}$, $f_{tp} = 13.311/Re_{tp}$
$\Delta P_{tp,a} = G^2\ x_{e,out}(1/\rho_g - 1/\rho_f)$

Author(s) [Ref.]	Viscosity models	MAE (%)
McAdams [16]	$1/\mu_{tp} = x_e/\mu_g + (1-x_e)/\mu_f$	55.78
Ackers et al. [17]	$\mu_{tp} = \mu_f/[(1-x_e)+x_e\sqrt{\rho_f/\rho_g}]$	59.11
Cicchitti et al. [18]	$\mu_{tp} = x_e\mu_g + (1-x_e)\mu_f$	77.19
Dukler et al. [19]	$\mu_{tp} = \rho_{tp}[x_e\mu_g/\rho_g + (1-x_e)\mu_f/\rho_f]$	55.02
Beattie and Whalley [20]	$\mu_{tp} = \omega\mu_g + (1-\omega)(1+2.5\omega)\mu_f$ $\omega = (x_e/\rho_g)/(1/\rho_f + x_e(1/\rho_g - 1/\rho_f))$	55.22
Lin et al. [21]	$\mu_{tp} = (\mu_f\mu_g/[\mu_g + x_e^{1.4}(\mu_f-\mu_g)]$	56.18

As explained above, acetone was pumped into the heat sink under a sub-cooled condition ($T_{in} < T_{sat}$). It is assumed that the acetone maintains a liquid state until it reaches zero thermodynamic equilibrium quality, $x_e = 0$. The flow is then converted to a saturated two phase mixture downstream from the location of zero quality. If the acetone can be converted into vapour within the micro-channels, the thermodynamic equilibrium quality reach 1, $x_e = 1$. Thus, the acetone will be converted to a superheated vapour. As illustrated in Fig. 4, each micro-channel in the heating area is divided into a single-phase liquid region $L_{sp,f}$, a two-phase region L_{tp}, and a single-phase vapour region $L_{sp,g}$.

The thermodynamic equilibrium quality is defined by

$$x_e = \frac{h - h_f}{h_{fg}}; \tag{2}$$

where, h_{fg} is the latent heat of evaporation.

According to energy conservation equation, the length of the single-phase liquid region can be determined by

$$L_{sp,f} = \frac{mc_{pf}L_h(T_{sat} - T_{in})}{Q}; \tag{3}$$

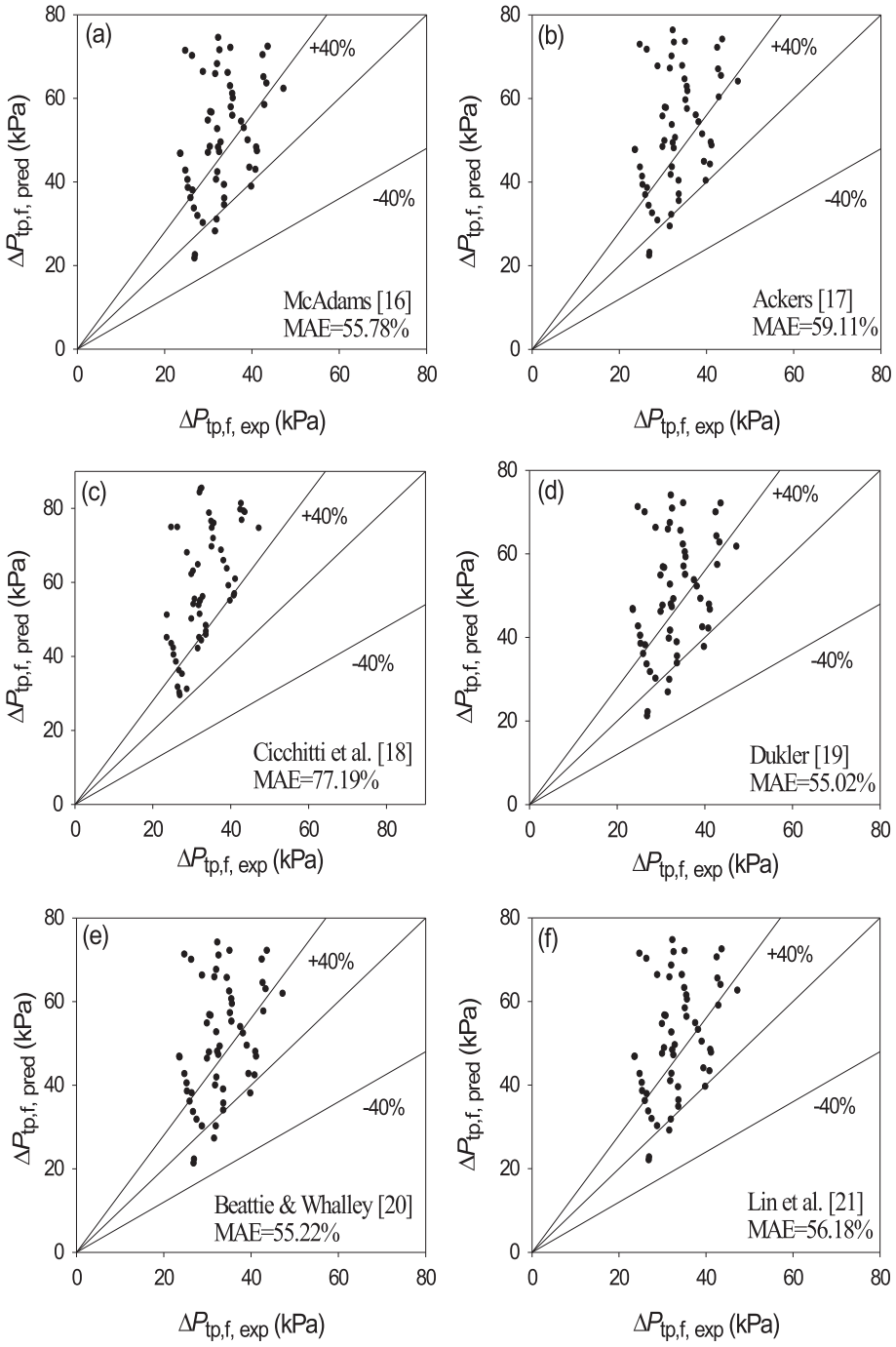

Fig. 5. Comparison of present pressure drop data with homogeneous equilibrium model predictions based on two-phase viscosity models by (a) McAdams, (b) Ackers, (c) Cicchitti et al., (d) Dukler, (e) Beattie and Whalley, and (f) Lin et al.

where, m is mass flux, c_{pf} is specific heat of capacity, T_{sat} is the saturated temperature relating to pressure, Q is effective heating power. As pointed out by Xu et al. [14], the ratio of the heat received by the fluid relative to total heating power is in the range of 0.77–0.90. Thus, we set the mean average value of 0.84 for the computation of the effective heating power. This yields a 6.5% uncertainty of the effective heating power.

If the acetone can be all converted into vapour, the length L_1 from inlet to the location of unity quality, $x_e = 1$, can be expressed by

$$L_1 = \frac{mc_{pf}L_h(T_{sat} - T_{in}) + h_{fg}}{Q}. \quad (4)$$

If the acetone cannot be converted into vapour completely in the heating area, there is no single-phase vapour section.

$$L_1 \geq L_h = 16 \quad (5)$$

$$L_{sp,g} = 0 \quad (6)$$

$$L_{tp} = L_h - L_{sp,f} \quad (7)$$

Else if the acetone can be converted into vapour completely in the heating area, the lengths of single-phase vapour region and two-phase region can be calculated, respectively by

$$L_{sp,g} = L_h - L_1 \quad (8)$$

$$L_{tp} = L_h - L_{sp,f} - L_{sp,g} \quad (9)$$

After calculating the length of two-phase region, the total pressure drop can be expressed as

$$\Delta P_{tot} = \Delta P_c + \Delta P_{in} + \Delta P_{sp,f} + \Delta P_{tp,f} + \Delta P_{tp,a} + \Delta P_{sp,g} + \Delta P_{out} - \Delta P_e \quad (10)$$

As we know, the two-phase frictional pressure drop is the main component of the total pressure drop, so the main object of present study is to calculate the two-phase frictional pressure drop,

$$\Delta P_{tp,f} = \Delta P_{tot} - \left(\Delta P_c + \Delta P_{in} + \Delta P_{sp,f} + \Delta P_{tp,a} + \Delta P_{sp,g} + \Delta P_{out} - \Delta P_e\right) \quad (11)$$

Table 6
Two-phase frictional pressure drop correlations based on SFM.

Author(s) [Ref.]	Correlations	MAE (%)
Lockhart and Martinelli [22]	$\Delta P_{tp,f} = 2G^2L_{tp}\int_{x_{e,in}}^{x_{e,out}}[f_f(1-x_e)\phi_f^2/\rho_f]dx_e/(d_h x_{e,out})$ $Re_f = G(1-x_e)d_h/\mu_f$, $f_f = 13.311/Re_f$ $\phi_f^2 = 1 + C/X_{vv} + 1/(X_{vv}^2)$, $C = 5$ $X_{vv}^2 = (\mu_f/\mu_g)[(1-x_e)/x_e](\rho_g/\rho_f)$ $Re_g = Gx_ed_h/\mu_g$ $\phi_f^2 = 1 + C/X_{vt} + 1/(X_{vt}^2)$, $C = 12$ $X_{vt}^2 = (f_fRe_g^{0.25}/0.079)[(1-x_e)/x_e](\rho_g/\rho_f)$	70.26
Chisholm [23]	$\Delta P_{tp,f} = 2f_{fo}G^2L_{tp}\int_{x_{e,in}}^{x_{e,out}}[\phi_{fo}^2]dx_e/(\rho_f d_h x_{e,out})$ $\phi_{fo}^2 = 1 + (\Gamma^2 - 1)[Bx_e^{0.5}(1-x_e)^{0.5} + x_e]$ $\Gamma^2 = (\mu_g/\mu_f)(\rho_f/\rho_g)$ When $\Gamma \leq 9.5$ and $G \leq 500$, B = 4.8	38.02

According to [15], some of the other components for triangular channel can be calculated by the equations shown in Table 4. When comparing it with the two-phase frictional pressure drop, the two-phase accelerational pressure drop is very small, which can be calculated by some models shown in the next section. Then, the experimental data of the two-phase frictional pressure drop will be obtained by equation (11).

3.2. Evaluation of previous correlations

The frictional pressure drop of two-phase flow can be predicted by the previous correlations, and the predictive capability of these models is given by the mean absolute error (MAE) as

$$MAE = \frac{1}{N}\sum\left[\frac{|\Delta P_{pred} - \Delta P_{exp}|}{\Delta P_{exp}} \times 100\right]. \quad (12)$$

3.2.1. Homogeneous equilibrium model

Table 5 shows the homogeneous equilibrium model (HEM) for predicting pressure drops of two-phase flow. A key unknown parameter for the calculation using HEM is the two-phase friction factor, f_{tp}, which is a function of the two-phase Reynolds number.

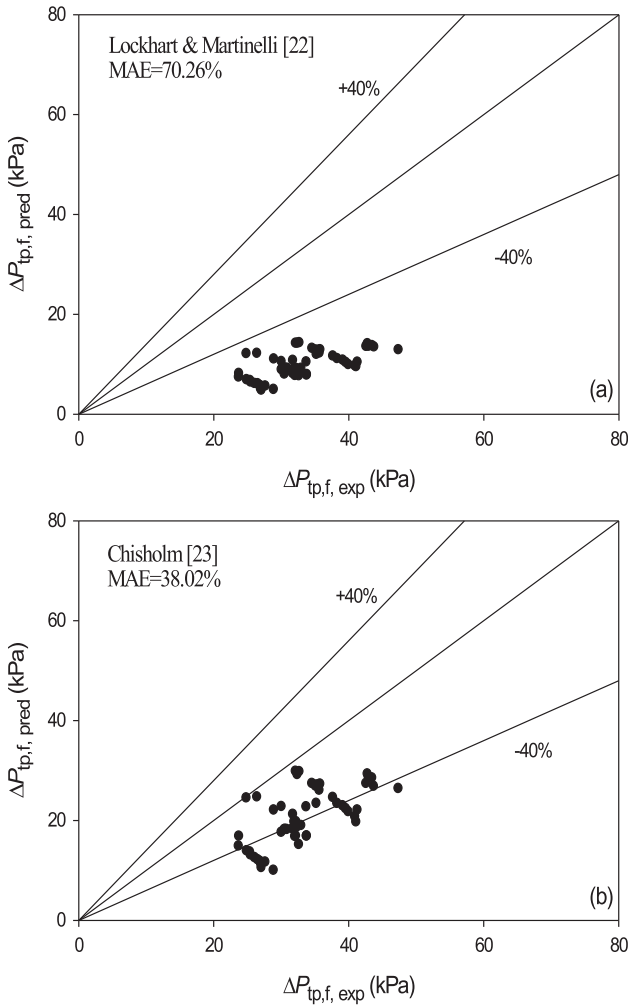

Fig. 6. Comparison of present pressure drop data with separated flow model predictions based on correlations by (a) Lockhart-Martinelli, (b) Chisholm.

The Reynolds number of two-phase flow is a function of two-phase viscosity, which depends on the models employed for calculations by different authors.

Fig. 5 shows that the HEM models mostly over predict present experimental data. And the MAE of the Cicchitti et al. [18] is bigger than that of the other models because this model is quality weighed and therefore provides significantly higher estimates of two-phase mixture viscosity at high vapour quality. All the other five models yield nearly deviation from the data with the MAE of about 55%.

3.2.2. Separated flow model

Table 6 shows two popular two-phase frictional pressure drop correlation for macro-channels based on separated flow model (SFM). The accelerational two-phase pressure drop was calculated by,

$$\Delta P_{tp,a} = G^2 \left[\frac{x_{e,out}^2}{\alpha_{out}} \left(\frac{\rho_f}{\rho_g} \right) + \frac{(1 - x_{e,out})^2}{1 - \alpha_{out}} - 1 \right] \Big/ \rho_f \quad (13)$$

where, the void fraction was determined from Zivi's relation [24]

$$\alpha = \left[1 + \left(\frac{1 - x_e}{x_e} \right) \left(\frac{\rho_g}{\rho_f} \right)^{2/3} \right]^{-1} \quad (14)$$

Fig. 6(a) shows Lockhart and Martinelli (LM) model [22] obviously under predict the present data. Interestingly, the prediction of the Chisholm macro-channel correlation [23] is not as poor as first thought. Fig. 6(b) illustrates that most of the data are in the range of 0 to −40%. With a MAE of 38.02%, this correlation yields the most accurate prediction of present data, comparing with all the previous correlations cited in present study.

As we know, the frictional pressure drop increases as hydraulic diameter decreases, while the pressure drop due to acceleration decreases. These differences in the macro-scale correlations are cause by turbulent flows for both liquid and vapour phases, but the liquid phase is often under the laminar condition in micro-scale.

3.2.3. Correlations for micro- and mini-channels

Table 7 gives several two-phase frictional pressure drop correlations for mini/micro scale channels. Fig. 7 shows the comparison of the measured frictional pressure drops with these correlations. It can be observed that Tran correlation [25] greatly overestimates the present experimental data. The Tran correlation was developed based on flow boiling in small channels with refrigerants R-134a at six different pressures ranging from 138 to 856 kPa. The used small channels were two sizes of round tubes (2.46 and 2.92 mm inside diameters) and one rectangular channel (4.06 × 1.7 mm). Tran et al. [25] used the confinement number, N_{conf}, which includes surface tension and hydraulic diameter to account for the maximum size of the bubble confined in small channel. The great deviation between this correlation and present data may caused by the differences in physical properties of R-134a and acetone, different pressure ranges, different channel shape and hydraulic diameter.

Fig. 7(b) and (c) shows that the correlations are all predict unusually small values compared to the present data. Qu and Mudawar [26] used water-cooled heat sink with 21 parallel 231 × 713 μm rectangular microchannels, and the experiment were preformed in the range of the outlet thermodynamic equilibrium quality not exceeding 0.2. They put forward a new correlation based on the Mishima and Hibiki [28] correlation by incorporating a mass velocity term. And the liquid phase and vapour phase were all laminar condition in their experiments and new correlation. But in present experiments, many cases are run at high vapour quality, and the vapour phase often reaches turbulent condition. So, a big deviation can be found between Qu and Mudawar correlation predictions and present experimental data.

Lee and Mudawar [27] carried out experiments using R-134a as working fluid under high outlet quality in 53 parallel 231 × 713 μm rectangular micro-channels. They assumed that the added complexity of two-phase flow in a micro-channel is the net result of interactions among liquid inertia, liquid viscous force, and surface tension. And the two-phase pressure drop multiplier was modified with a new dimensionless parameter defined as a function of the Reynolds and Weber numbers. But the correlation still cannot predict present data well, due to large differences between the thermophyscial properties of the two coolants and the micro-channels with different geometries and hydraulic diameters.

Table 7
Two-phase frictional pressure drop correlations for mini/micro scale channels.

Author(s) [Ref.]	Correlations	MAE (%)
Tran et al. [25]	$\Delta P_{tp,f} = 2 f_{fo} G^2 L_{tp} \int_{x_{e,in}}^{x_{e,out}} \phi_{fo}^2 dx_e / (\rho_f d_h x_{e,out})$ $\phi_{fo}^2 = 1 + (4.3 I^2 - 1)[N_{conf} x_e^{0.875} (1 - x_e)^{0.875} + x_e^{1.75}]$ $I^2 = (\mu_g/\mu_f)(\rho_f/\rho_g)$ $N_{conf} = \left[\frac{\sigma}{g(\rho_f - \rho_g)} \right]^{0.5} / d_f$	194.20
Qu and Mudawar [26]	$\Delta P_{tp,f} = 2 G^2 L_{tp} \int_{x_{e,in}}^{x_{e,out}} [f_f (1 - x_e) \phi_f^2 / \rho_f] dx_e / (d_h x_{e,out})$ $Re_f = G(1 - x_e) d_h / \mu_f$, $f_f = 13.311 / Re_f$ $\phi_f^2 = 1 + C/X_{vv} + 1/(X_{vv}^2)$ $C = 21 \times [1 - \exp(-0.319 \times 10^3 d_h)](0.00418\, G + 0.0613)$ $X_{vv}^2 = (\mu_f/\mu_g)[(1 - x_e)/x_e](\rho_g/\rho_f)$	84.47
Lee and Mudawar [27]	$\Delta P_{tp,f} = 2 G^2 L_{tp} \int_{x_{e,in}}^{x_{e,out}} [f_f (1 - x_e) \phi_f^2 / \rho_f dx_e] / (d_h x_{e,out})$ $Re_f = G(1 - x_e) d_h / \mu_f$, $f_f = 13.311 / Re_f$ $Re_{fo} = G d_h / \mu_f$, $We_{fo} = G^2 d_h / (\sigma \rho_f)$ $\phi_f^2 = 1 + C/X + 1/(X^2)$ $C_{vv} = 2.16\, Re_{fo}^{0.047}\, We_{fo}^{0.60}$ (laminar liquid-laminar vapour) $C_{vt} = 1.45 Re_{fo}^{0.25} We_{fo}^{0.23}$ (laminar liquid-turbulent vapour)	81.75

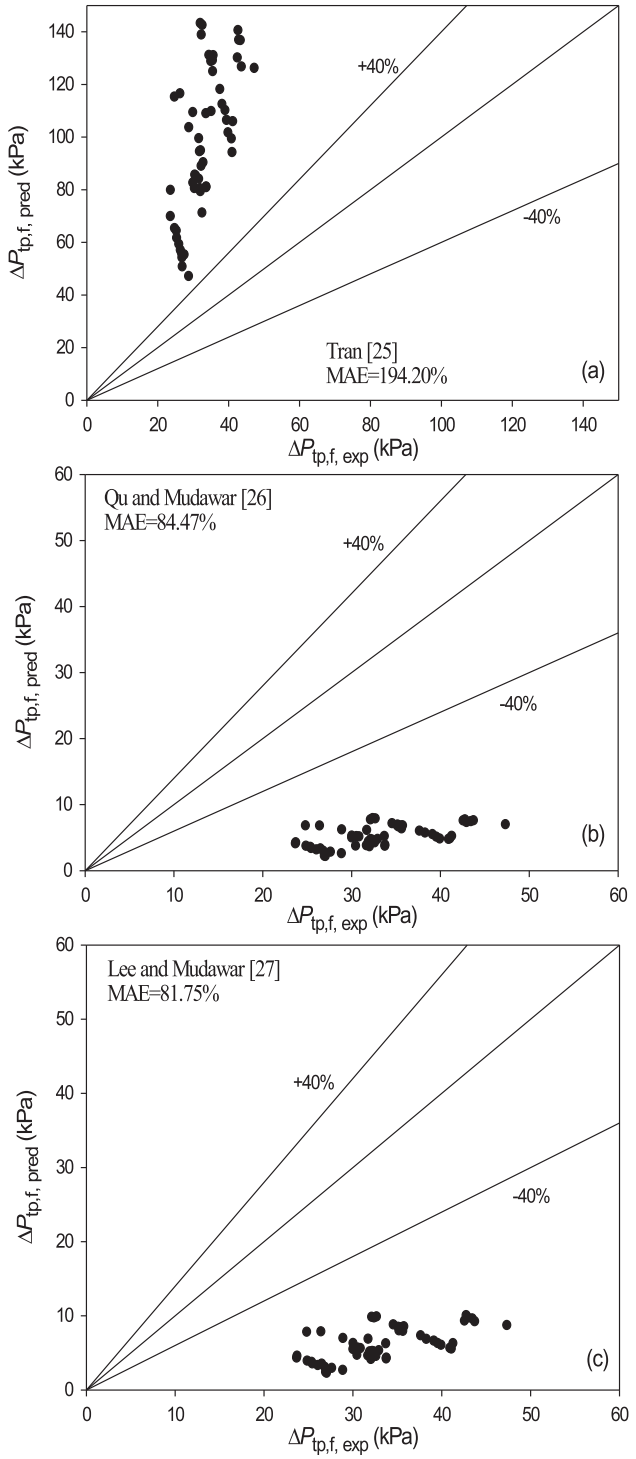

Fig. 7. Comparison of pressure drop data with predictions of mini/micro-channel correlations of (a) Tran et al., (b) Qu and Mudawar, and (c) Lee and Mudawar.

4. New correlation

According to the above discussion, all these correlations based on HEM or SFM models for macro scale or mini/micro scale channels, cannot predict present experimental data accurately. Compared with all other correlations, the classical Chisholm correlation can predict present data with the smallest MAE of 38.02%. In an effort to improve predictive accuracy, the authors of the present study modified the Chisholm correlation, as shown in Table 8. The parameter B in the new correlation was regressed as a function of mass flux G based on present data. And Fig. 8 shows the effectiveness of the new correlation at predicting the present two-phase frictional pressure drop data with a MAE of 12.56%.

Table 8
New correlation based on modified Chisholm model.

Author(s)	Correlations	MAE (%)
Present study	$\Delta P\mathrm{tp,f} = 2f_{\mathrm{fo}}G^2L_{\mathrm{tp}}\int_{x_{\mathrm{e,in}}}^{x_{\mathrm{e,out}}}[\phi_{\mathrm{fo}}^2]dx_{\mathrm{e}}/(\rho_{\mathrm{f}}d_{\mathrm{h}}x_{\mathrm{e,out}})$ $\phi_{\mathrm{fo}}^2 = 1+(\Gamma^2-1)[Bx_{\mathrm{e}}^{0.5}(1-x_{\mathrm{e}})^{0.5}+x_{\mathrm{e}}]$ $\Gamma^2 = (\mu_{\mathrm{g}}/\mu_{\mathrm{f}})(\rho_{\mathrm{f}}/\rho_{\mathrm{g}})$ $B = 169.6258\ G^{-0.5747}$	12.56

5. Main characteristics of two-phase pressure drop

Though, it is a very common phenomenon of two-phase flow instabilities, such as pressure drop type oscillation in macro scale. In present study, the very stable fluid pressure signals were found due to the response time of the pressure sensor is longer than the cycle period of transient explosive boiling in silicon micro-channels which is at millisecond time scale [14,29]. Thus, the present experimental data are representative of the stable flow boiling.

In order to explore the dominant features of two-phase pressure drop, the individual components of the total pressure drop were calculated, and two typical cases were shown by Fig. 9. The two-phase frictional pressure drop occupied the biggest part of the total pressure drop, and the second one is the two-phase accelerational pressure drop. When the exit thermodynamic equilibrium quality exceeds unity, the two-phase accelerational pressure drop may increase greatly.

It is well known that the two-phase frictional pressured drop characteristics deeply depend on flow pattern. Four typical flow patterns have been identified by Xu et al. [14], liquid plug/vapour slug flow, inverse bubble slug entrained in the liquid plug flow, paired or triplet bubbles entrained in liquid plug and transient annular flow. Even when the mean exit thermodynamic equilibrium quality is larger than unity, the transient flow patterns also happened in the micro-channels with slightly superheated outlet vapour. The bubble nucleation, growth and coalescence can still be identified. So some correlations for micro-channels based on annular flow pattern [26,27] failed to predict the present data. And it is not difficult to explain that all the previous correlations give

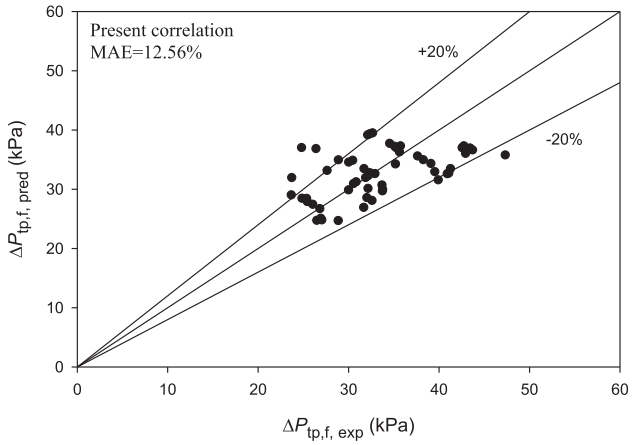

Fig. 8. Comparison of present correlation predictions with pressure drop data.

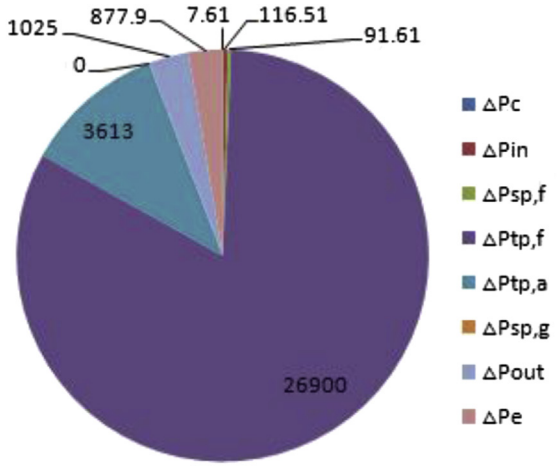

(a) T_{in} =23 °C, ΔP_{tot} =30.8759kPa, Q=17.0W, G=97.25 kg/m^{2}s, x_e=0.9172

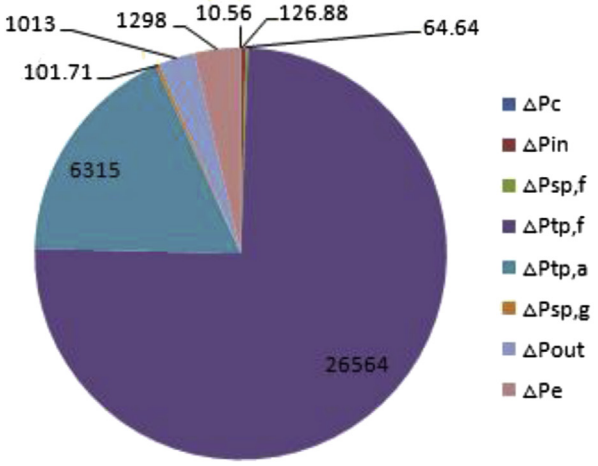

(b) T_{in} =32.7 °C, ΔP_{tot} =32.8982kPa, Q=24.0W, G=113.71 kg/m^{2}s, x_e=1.1834

Fig. 9. Individual components of pressure drop (all units are Pa).

unsatisfied predictions of present experimental data. Not only because so many factors should be considered, such as different hydraulic diameter, materials, geometry of micro-channels, working fluids, and working conditions, but also the particular flow pattern and heat transfer mechanism.

The particular explosive flow boiling and transient flow pattern at micro time scale bring more complexity into the accurate prediction of present two-phase frictional pressure drop [30]. That is the main objective of present study to put forward a new correlation based on present data. Fortunately, it is obtained using the regress method based on the classical Chisholm model. Future works are suggested to be performed experimentally and theoretically using more working fluids and under different conditions, in order to reach more universal and accurate predictions.

Tang et al. [31,32] thought that surface roughness may have significant effect on the pressure drop in microchannel flow, even just larger than 1%. It should be noted that the smooth silicon micro-channels have nanoscale surface roughness, at least two orders to three orders of magnitude less than the conventional miniature channels fabricated with metallic material such as copper and stainless steel. In present study, the silicon microchannels were etched and the surface roughness was not bigger than 10 nm. So the relative surface roughness is less than 0.00064, and the effect of surface roughness cannot be considered. Some recent researches also treated the channels with a relative roughness range of 0.001–0.0001 as smooth tubes [33,34].

6. Conclusions

The characteristics of two-phase frictional pressure drop has been investigated experimentally in parallel triangular silicon micro-channels using acetone as working fluid at high exit thermodynamic equilibrium quality. Both homogeneous equilibrium and separated flow models have been evaluated, and a new correlation has been put forward to improve the overall predictive accuracy. The following can be concluded:

(1) The homogeneous equilibrium model with six popular two-phase viscosity models all generally over predicted the present acetone data.
(2) The Lockhart and Martinelli model obviously under predict the present data.
(3) The classical Chisholm model yields prediction of present data with a MAE of 38.02%.
(4) There are great deviations between the predictions of several correlations for mini/micro scale channels and present data.
(5) The correlation errors occur due to not only the different hydraulic diameter, materials, geometry of channels,

working fluids, and working conditions, but also the particular two-phase flow pattern and flow boiling mechanisms.

(6) The new correlation model is presented to predict the frictional pressure drops in two-phase flow boiling for microchannels, in which the Chisholm constant B is given as a function of mass flux. The newly suggested correlation satisfactorily predicts the present acetone data within MAE of 12.56%.

Acknowledgements

The research is supported by the National Natural Science Foundation of China (No. 51376066, 51211130118), Int. Cooperation Project (No. 51210011), Royal Society-NSFC Joint Project (IE110858), the special foundation of Pearl River New Star of Science and Technology in Guangzhou City (No. 2012J220002) and Guangdong Province Key Laboratory of Efficient and Clean Energy Utilization, South China University of Technology (No. 2013A061401005).

References

[1] S. Szczukiewicz, M. Magnini, J.R. Thome, Proposed models, ongoing experiments, and latest numerical simulations of microchannel two-phase flow boiling, Int. J. Multiph. Flow 59 (2014) 84–101.
[2] S. Gedupudi, Y.Q. Zu, T.G. Karayiannis, et al., Confined bubble growth during flow boiling in a mini/micro-channel of rectangular cross-section part I: experiments and 1-D modelling, Int. J. Therm. Sci. 50 (2011) 250–266.
[3] Y.Q. Zu, Y.Y. Yan, S. Gedupudi, et al., Confined bubble growth during flow boiling in a mini/micro-channel of rectangular cross-section part II: approximate 3-D numerical simulation, Int. J. Therm. Sci. 50 (2011) 267–273.
[4] J.L. Xu, Y.H. Gan, Uniform MEMS chip temperatures in the nucleate boiling heat transfer region by selecting suitable, medium boiling number range, Nanosc. Microsc. Therm. 11 (2007) 273–300.
[5] J.L. Xu, Y.H. Gan, D.C. Zhang, et al., Microscale heat transfer enhancement using thermal boundary layer redeveloping concept, Int. J. Heat Mass Transfer 48 (2005) 1662–1674.
[6] W. Yu, D.M. France, M.W. Wambsganss, et al., Two-phase pressure drop, boiling heat transfer, and critical heat flux to water in a small-diameter horizontal tube, Int. J. Multiph. Flow 28 (2002) 927–941.
[7] L. Sun, K. Mishima, Evaluation analysis of prediction methods for two-phase flow pressure drop in mini-channels, Int. J. Multiph. Flow 35 (2009) 47–54.
[8] P. Lee, S.V. Garimella, Saturated flow boiling heat transfer and pressure drop in silicon microchannel arrays, Int. J. Heat Mass Transfer 51 (2008) 789–806.
[9] T. Phan, H. Caney, N. Marty, et al., Flow boiling of water in a minichannel: the effects of surface wettability on two-phase pressure drop, Appl. Therm. Eng. 31 (2011) 1894–1905.
[10] D. Brutin, V.S. Ajaev, L. Tadrist, Pressure drop and void fraction during flow boiling in rectangular minichannels in weightlessness, Appl. Therm. Eng. 51 (2013) 1317–1327.
[11] B. Fu, M. Tsou, C. Pan, Flow-pattern-based correlations for pressure drop during flow boiling of ethanol–water mixtures in a microchannel, Int. J. Heat Mass Transfer 61 (2013) 332–339.
[12] G. Ribatski, L. Wojtan, J.R. Thome, An analysis of experimental data and prediction methods for two-phase frictional pressure drop and flow boiling heat transfer in micro-scale channels, Exp. Therm. Fluid Sci. 31 (2006) 1–19.
[13] C.L. Yaws, Chemical Properties Handbook, McGraw-Hill, 1999.
[14] J.L. Xu, Y.H. Gan, D.C. Zhang, et al., Microscale boiling heat transfer in a microtimescale at high heat fluxes, J. Micromech. Microeng. 15 (2005) 362–376.
[15] W.M. Rohsenow, J.P. Hartnett, Y.I. Cho, Handbook of Heat Transfer, third ed., McGraw-Hill Professional, 1998.
[16] W.H. McAdams, Heat Transmission, third ed., McGraw-Hill, New York, 1954.
[17] W.W. Akers, H.A. Deans, O.K. Crosser, Condensing heat transfer within horizontal tubes, Chem. Eng. Prog. 54 (1958) 89–90.
[18] A. Cicchitti, C. Lombardi, M. Silvestri, et al., Two-phase cooling experiments pressure drop, heat transfer and burnout measurement, Energ. Nucl. 7 (1960) 407–425.
[19] A.E. Dulker, M. Wicks III, R.G. Cleveland, Frictional pressure drop in two-phase flow: A. A comparison of existing correlations for pressure loss and holdup, J. AIChE 10 (1964) 38–43.
[20] D.R.H. Beattie, P.B. Whalley, A simple two-phase frictional pressure drop calculation method, Int. J. Multiph. Flow 8 (1982) 83–87.
[21] S. Lin, C.C.K. Kwok, R.Y. Li, et al., Local frictional pressure drop during vaporization of R-12 through capillary tubes, Int. J. Multiph. Flow 17 (1991) 95–102.
[22] R.W. Lockhart, R.C. Martinelli, Proposed correlation of data for isothermal two-phase, two-component flow in pipes, Chem. Eng. Prog. 45 (1949) 39–48.
[23] D. Chisholm, Pressure gradients due to friction during the flow of evaporation two-phase mixtures in smooth tubes and channels, Int. J. Heat Mass Transfer 16 (1973) 347–358.
[24] S.M. Zivi, Estimation of steady-state stem void-fraction by means of the principle of minimum entropy production, ASME J. Heat Transfer 86 (1964) 247–252.
[25] T.N. Tran, M.C. Chyu, M.W. Wambsganss, et al., Two-phase pressure drop of refrigerants during flow boiling in small channels: an experimental investigation and correlation development, Int. J. Multiph. Flow 26 (2000) 1739–1754.
[26] W.L. Qu, I. Mudawar, Measurement and prediction of pressure drop in two-phase micro-channel heat sinks, Int. J. Heat Mass Transfer 46 (2003) 2737–2753.
[27] J. Lee, I. Mudawar, Two-phase flow in high-heat-flux micro-channel heat sink for refrigeration cooling applications: Part I-pressure drop characteristics, Int. J. Heat Mass Transfer 48 (2005) 928–940.
[28] K. Mishima, T. Hibiki, Some characteristics of air-water two-phase flow in small diameter vertical tubes, Int. J. Multiph. Flow 22 (1996) 703–712.
[29] Y.H. Gan, J.L. Xu, S.F. Wang, Are the available boiling heat transfer coefficients suitable for silicon microchannel heat sinks? Microfluid. Nanofluid. 4 (2008) 575–587.
[30] J.L. Xu, S. Sheng, Y.H. Gan, et al., Transient flow pattern based microscale boiling heat transfer mechanisms, J. Micromech. Microeng. 15 (2005) 1344–1361.
[31] G.H. Tang, Z. Li, Y.L. He, et al., Experimental observations and lattice Boltzmann method study of the electroviscous effect for liquid flow in microchannels, J. Micromech. Microeng. 17 (2007) 539–550.
[32] G.H. Tang, Z. Li, Y.L. He, et al., Experimental study of compressibility, roughness and rarefaction influences on microchannel flow, Int. J. Heat Mass Transfer 50 (2007) 2282–2295.
[33] S.M. Kim, I. Mudawar, Universal approach to predicting two-phase frictional pressure drop for adiabatic and condensing mini/micro-channel flows, Int. J. Heat Mass Transfer 55 (2012) 3246–3261.
[34] S.M. Kim, I. Mudawar, Universal approach to predicting two-phase frictional pressure drop for mini/micro-channel saturated flow boiling, Int. J. Heat Mass Transfer 58 (2013) 718–734.